

# Validation of *FLOW-3D* against a 3D Dam Breaking Problem

Peter Arnold, Minerva Dynamics, The Guildhall, High Street Bath, UK

## Introduction

A 3D dam breaking with obstacle configuration was chosen as one of our *FLOW-3D*<sup>1</sup> validation cases in order to assess *FLOW-3D*'s performance for the simulation of free-surface flows. The problem is well documented and easy to set up with all the experimental data generated available to download from the ERCOFTAC database[1]. The obstacle is chosen to be representative of a container exposed to green water on the deck of a ship. Videos of the experiment and SPH simulations (smoothed particle hydrodynamics) are available in the database that show impressive qualitative agreement. The experiment consists of a large tank 3.22m x 1m x 1m with a sliding door holding back 0.55m of water. The door is opened vertically upwards by a falling weight and the water is released to impinge on the obstacle and then be reflected from the tank walls 3 times. The free-surface elevation is measured at four locations along the center line of the tank and eight pressure sensors are embedded in the leading vertical and horizontal surfaces of the obstacle. CFD simulations using *FLOW-3D* v9.4 were carried out on a series of progressively finer meshes and using different order numerical schemes and turbulence models.

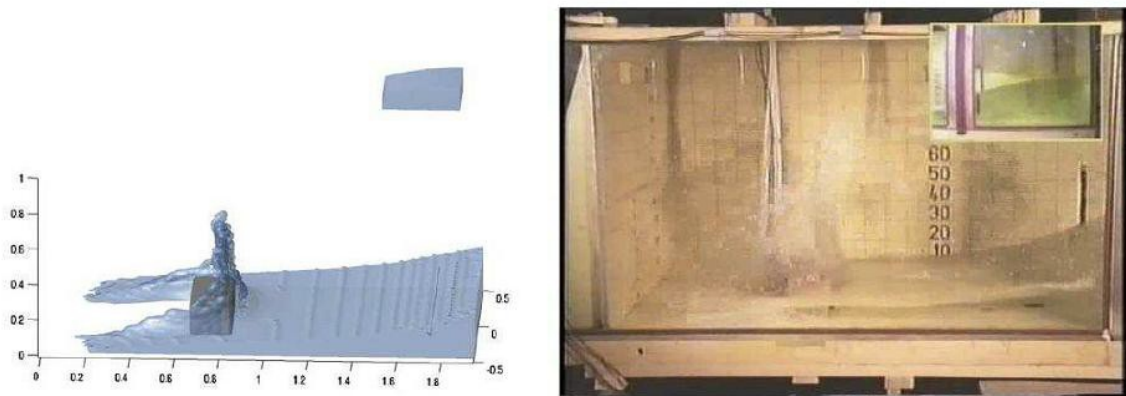


Figure 1. Snapshot of SPH simulation and experiment at 0.56 secs

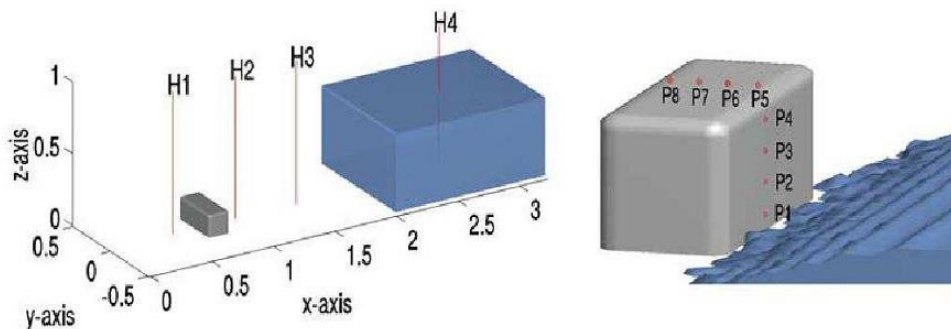


Figure 2. Locations of water height and pressure measurements

<sup>1</sup> *FLOW-3D* is a registered trademark of Flow Science, Inc. in the USA and other countries.

## Simulation Methodology

The 3D dam breaking problem was originally developed by Kleefsman et al. [2.] Full details of the locations of the sensors and the experimental data and videos of the experiment and an SPH simulation are available in the EROFTAC validation database [1]. The simulation is carried out for a total of 6 seconds of real time.

The **FLOW-3D** simulations were set up for a domain of 3.22m x 1m X 1.5m, i.e., 0.5 larger in the z-direction to allow any vertical jets of fluid to be captured (in the experiment the tank roof is open to atmosphere). The default mesh had hexahedral cells with a spacing of 161 in the x-direction, 50 in the y-direction and 75 in the z-direction and was uniformly spaced other than for accommodating fixed points to coincide with the obstacle and sensor locations, hence a total of approximately 603,750 cells. The obstacle was put into the domain and all walls were treated as no slip. After prescribing the initial location of the water and its viscosity, laminar time-dependent simulations were carried out for a series of progressively finer meshes starting from the default 603K cell mesh (Mesh 1). The approach taken was simply to increase the total cell count by a factor of two for each progressive mesh by increasing the number of cells in each direction by the cube root of 2. Four meshes were generated in this way, i.e., Mesh 1, Mesh 2, Mesh 3 and Mesh 4. The time histories of the free-surface elevation at four locations and the pressure from the eight pressure sensors were then plotted against the experimental data. The CPU and elapsed time of the four processors was also recorded.

Using only Mesh 1, the effects of the numerical differencing scheme used for the momentum advection was investigated. The default 1st order, a 2nd order monotonicity preserving and a 3rd order scheme were all used and the results compared. Also the effects of running in single and double precision were compared. Finally a mesh was designed ( Mesh 5) to capture the velocity gradient along the bottom wall and the bulk flow in the most active parts of the domain using  $2.7 \times 10^6$  active cells.

The turbulent fluctuations were modeled primarily by direct simulation, however, we have also included the results from two of the turbulence models available in **FLOW-3D**, i.e., the Renormalization Group (RNG) Model and the Large Eddy Simulations (LES ) model. All models were run on the coarsest mesh, i.e., Mesh 1 only. We have not attempted to satisfy the usual turbulence model associated constraints on the distance of the nearest node from the tank walls due to the excessive demands this would put on the mesh resolution. Also as the flow is largely chaotic and the obstacle is sharp edged the prediction of the flow separation effects will be driven by the rapid changes in geometry rather than by a gradual separation of an orderly boundary layer. Consequently, we have assumed that resolution of the boundary layer is less relevant than resolving the flow in the interior of the domain from the viewpoint of predicting the main flow features.

## Results

**Table 1.** CPU and Elapsed Times for Each Mesh and Method

Mesh	Number of Cells	Momentum Advection	Single/Double Precision	Turbulence Model	Elapsed Time of Four Processors	CPU Time (secs)
Mesh 1	$6.03 \times 10^5$	1st Order	Single	Laminar	971	3389
Mesh 2	$1.22 \times 10^6$	1st Order	Single	Laminar	2227	8223
Mesh 3	$2.39 \times 10^6$	1st Order	Single	Laminar	7951	30710
Mesh 4	$4.84 \times 10^6$	1st Order	Single	Laminar	19330	72780
Mesh 5	$2.73 \times 10^6$	1st Order	Single	Laminar	32780	130200
Mesh 1	$6.03 \times 10^5$	2nd Order	Single	Laminar	1168	4186
Mesh 1	$6.03 \times 10^5$	3rd Order	Single	Laminar	1232	4456
Mesh 1	$6.03 \times 10^5$	1st Order		Laminar	1039	3646
Mesh 1	$6.03 \times 10^5$	2nd Order	Single	RNG	2004	7538
Mesh 1	$6.03 \times 10^5$	2nd Order	Single	LES	1253	4539

## Free-Surface Elevation Results

Figures 3-6 show the free-surface elevation plotted against time at each of the four locations with H4 being nearest and H1 being furthest from the original water column. It is encouraging for the validation that the main features are represented very well albeit with some differences in magnitude and timing. However, it must also be said that the experimental data has no error bars supplied with it and that the measurement of the free-surface elevation using probes in such a chaotic and separated flow field is likely to be problematic as the free-surface elevation may not be a single valued function of time. This probably accounts for the discrepancy in the H1 heights during the initial steep rise phase at around 1 second. The remainder of the H1 record is in good agreement with the experiments. The H2 plot shows even better agreement particularly in the initial water rising phase and predicts well the eventual maximum height of the water. The H3 plot again picks up the main characteristics but clearly shows a time lag between the simulations and experiment. The H4 plot shows excellent agreement in the initial phase as the water level is decreasing but underestimates the steepness and final values of the rise of the water column as it returns off the left and right hand walls respectively.

The time lag feature of the simulations behind the experiment is present in all the plots and is also seen in the original CFD simulation by Kleefsman et al. [2] using their CoMFLOW code on a 236 X 76 X 68 grid and so cannot be attributed to **FLOW-3D** alone. The origin of the lag is unclear but it seems to be introduced gradually over the simulation.

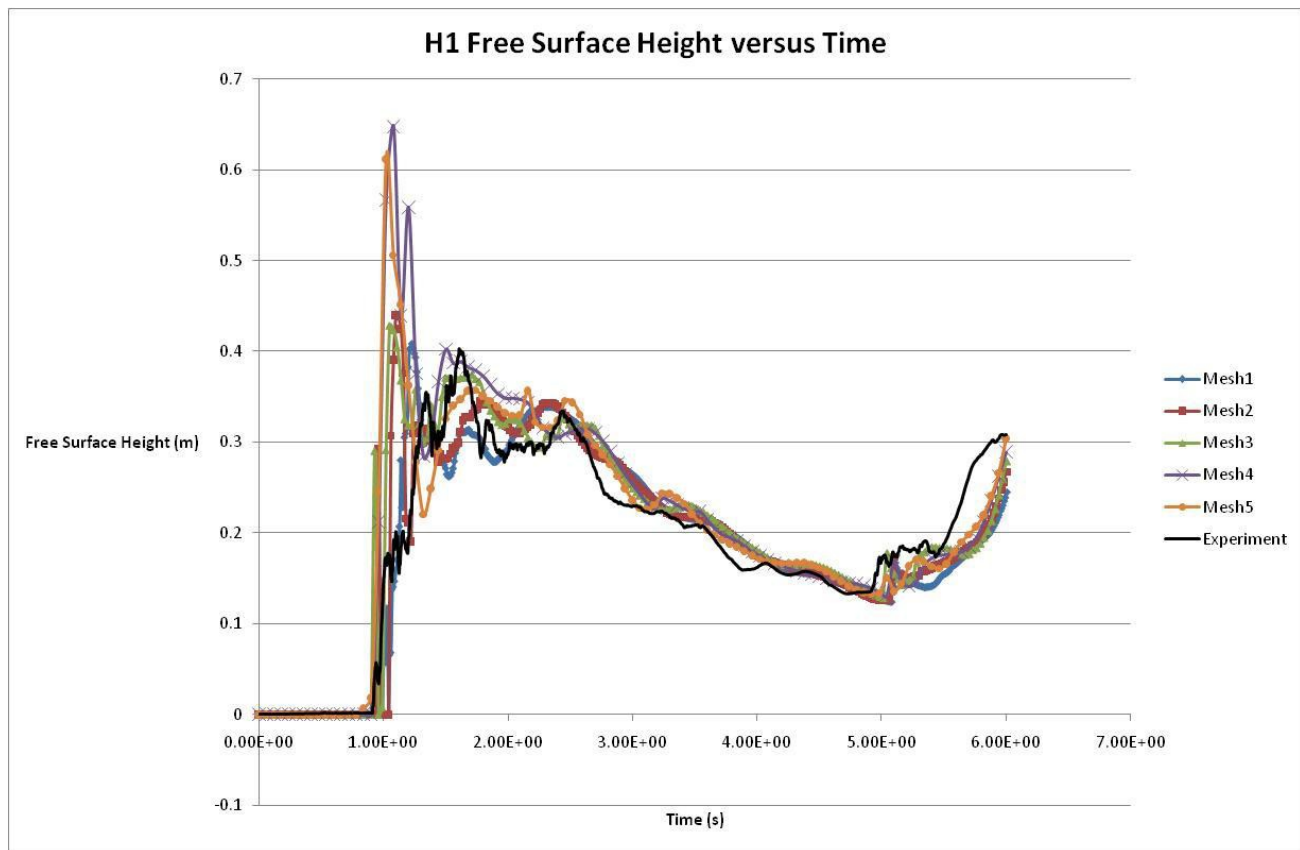


**Figure 3.** Free-surface height at location H1

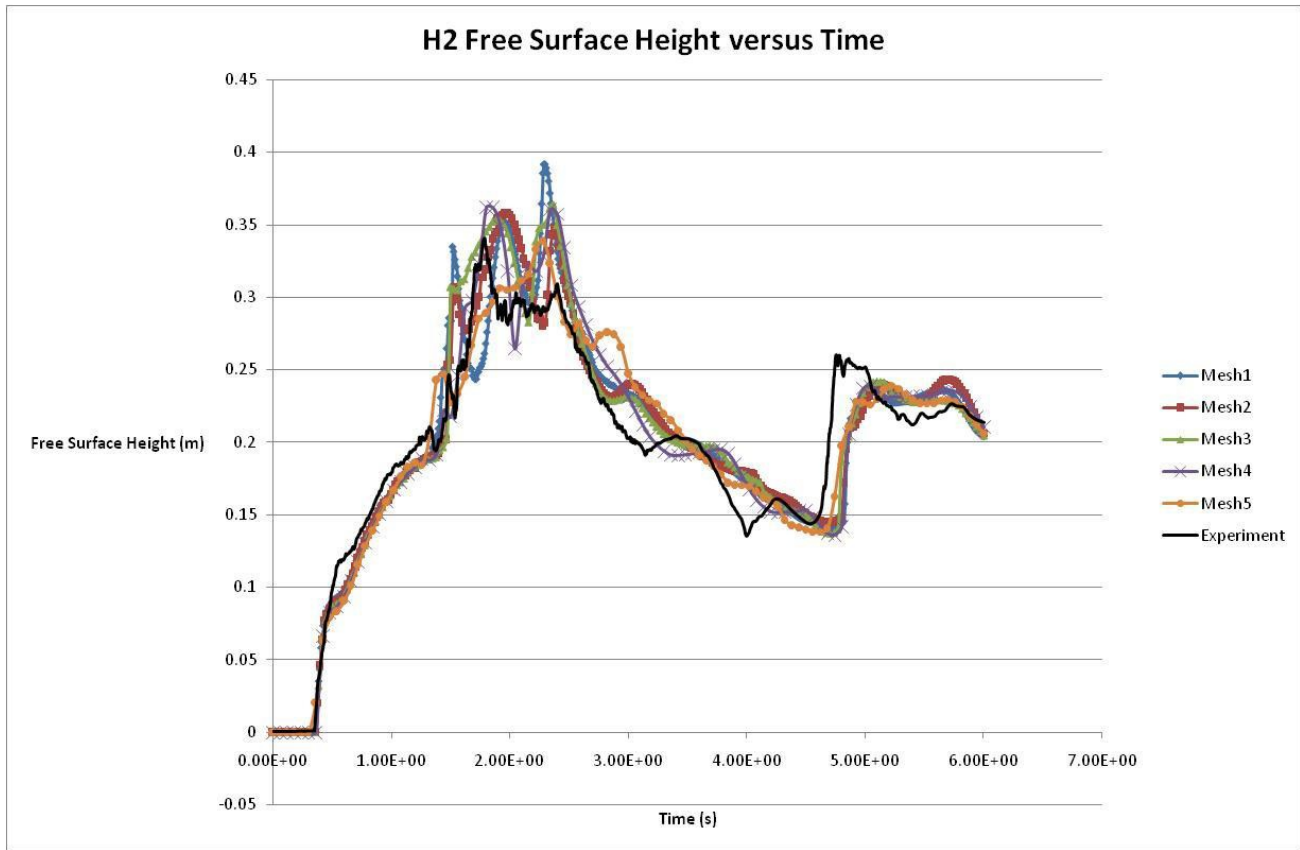


**Figure 4.** Free-surface height at location H2

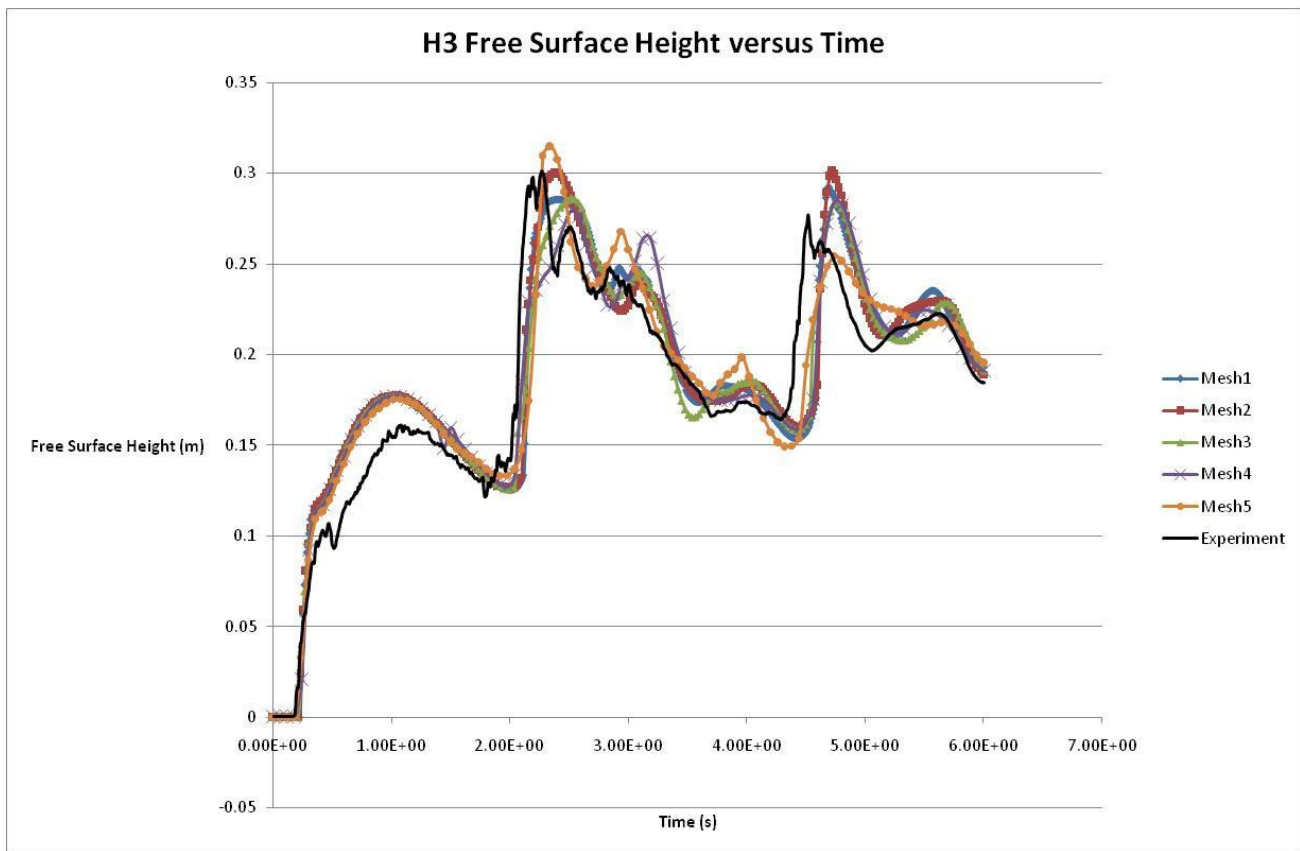


**Figure 5.** Free-surface height at location H3

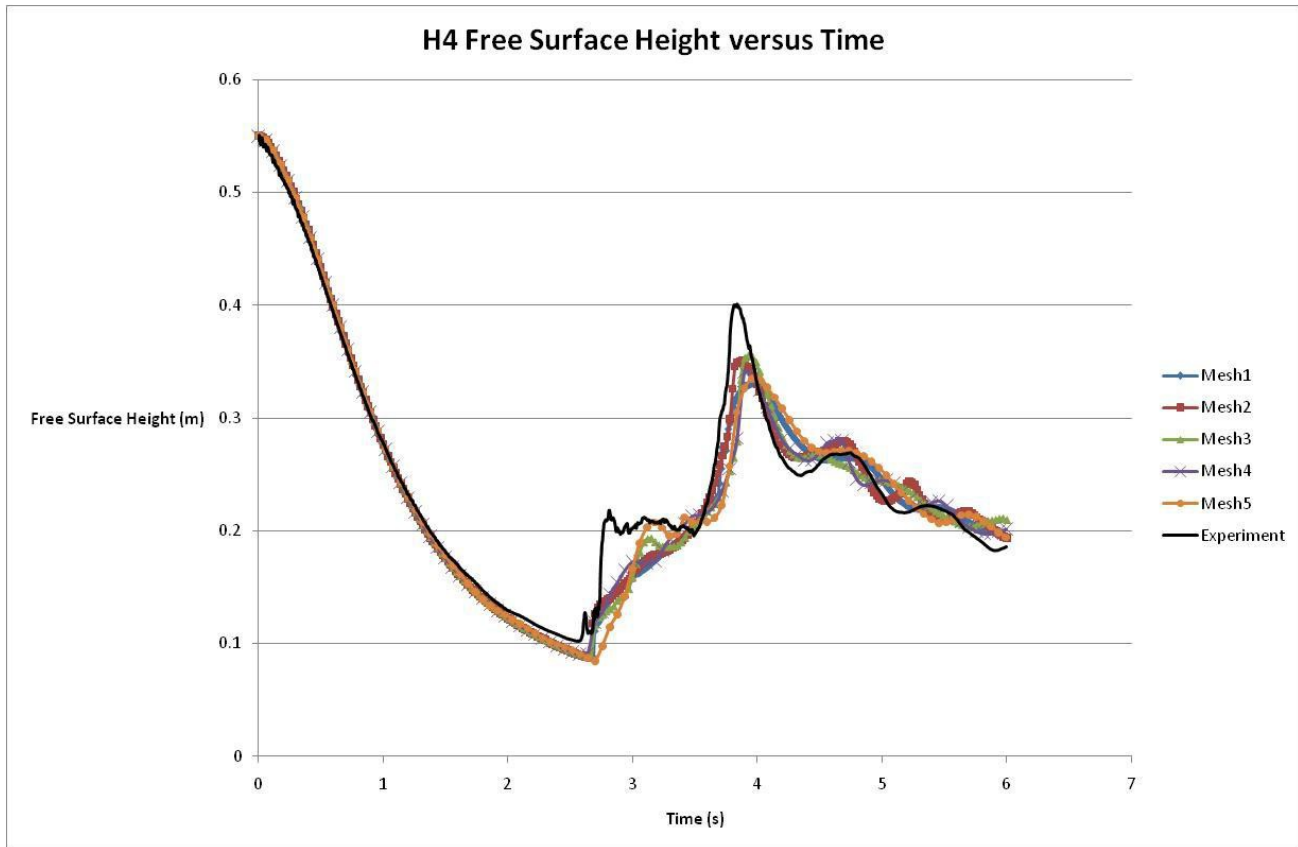


**Figure 6.** Free-surface height at location H4

### Pressure Sensors Results

Figures 7-10 show the four front face pressure sensors plotted against time, indicating generally good agreement between experiment and the simulations with the accuracy increasing for the pressure sensors located towards the floor of the tank. The P1 sensor estimates the arrival and magnitude of the pressure peak the most accurately. There is a considerable amount of fluctuation in the pressure signal between its arrival and about 2 seconds as the water rebounds from the obstacle and left wall after which the signal settles down and the simulations values agree well with the experimental values. Also the magnitude of the peak decrease with the height up the face of the sensor. The worst agreement occurs as we would expect at the P4 location where flow separation is taking place.

Figures 11-14 show the top horizontal face pressure sensors, i.e., P5 to P8 also show along with experimental data, large fluctuations in pressure between 1 and 2 seconds after which again the simulations and experimental data settle down and agreement is improved. The CoMFLOW simulations performed by Kleefsman et al. [2] show similar characteristics and levels of agreement but overestimate the pressure peaks along the top face considerably more.

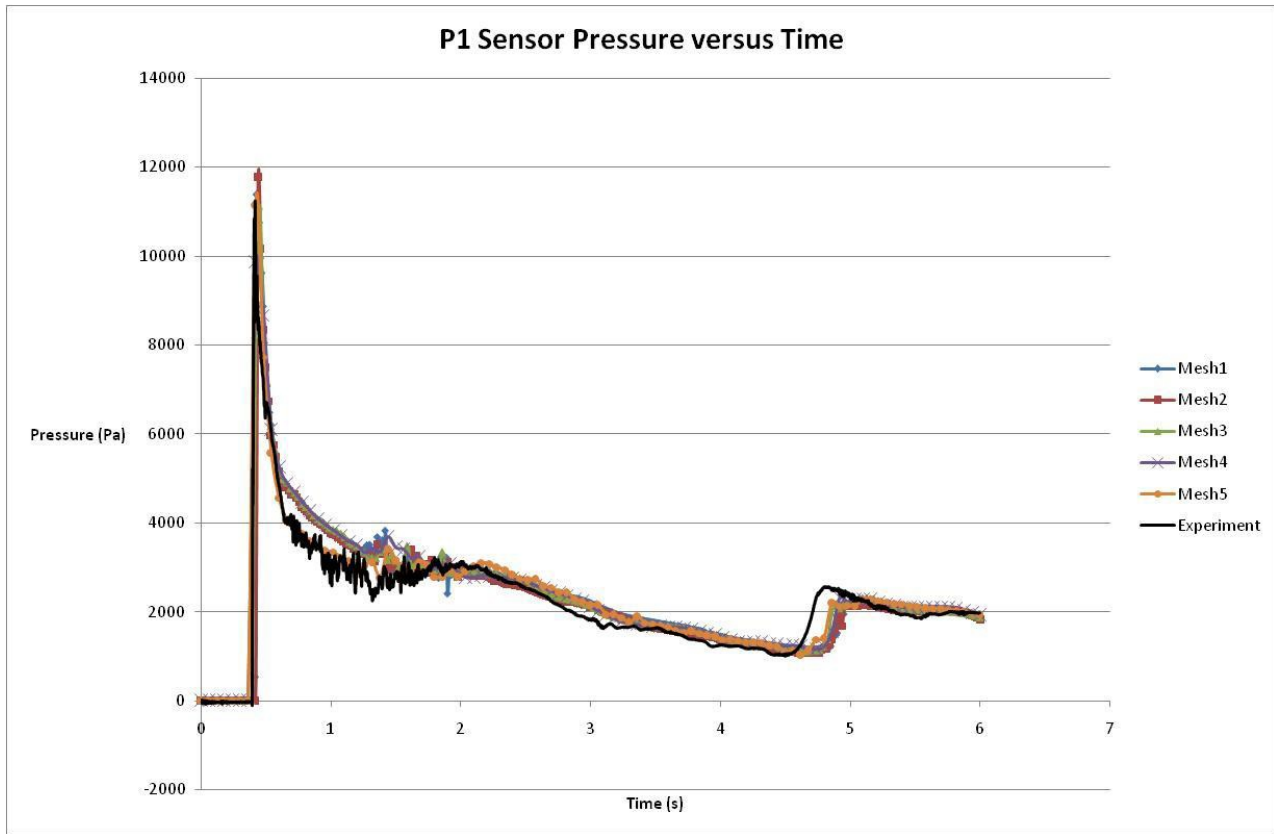


**Figure 7.** Pressure at location P1

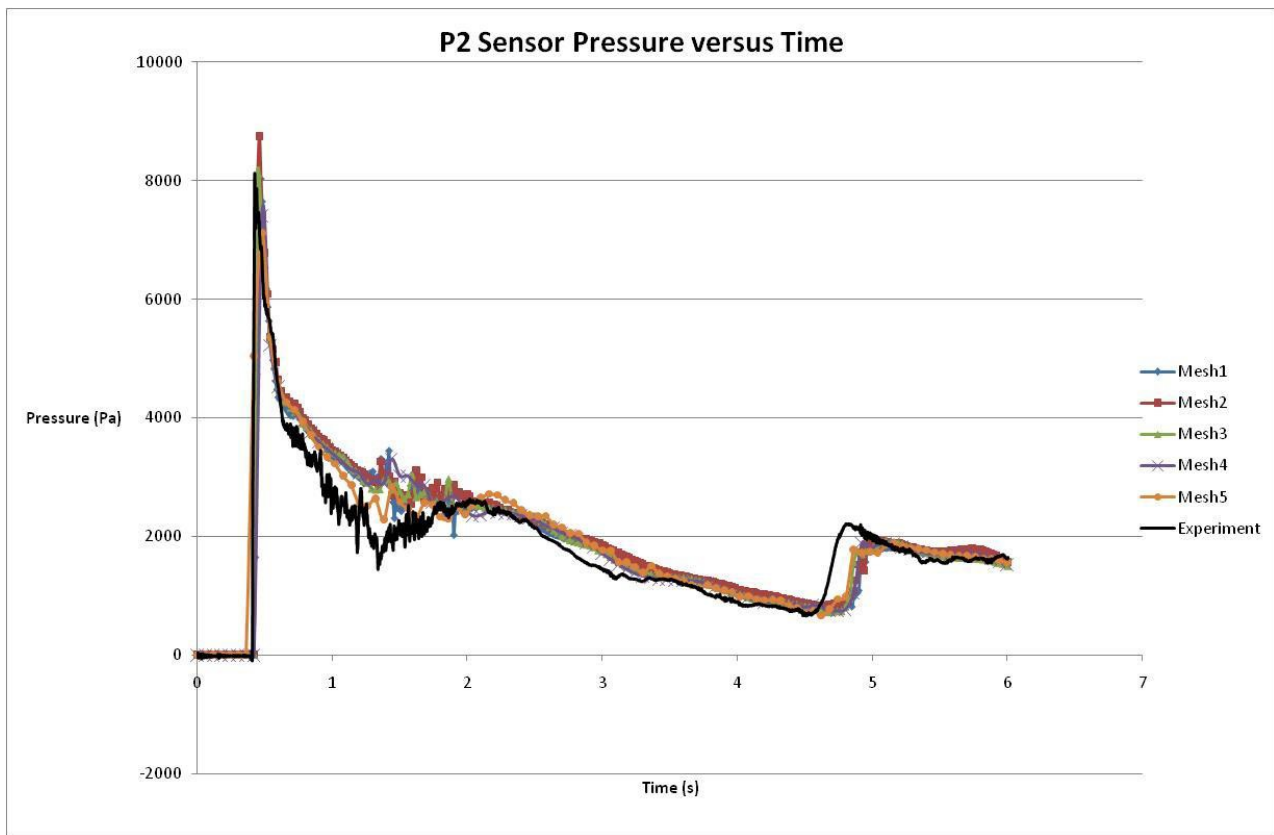


**Figure 8.** Pressure at location P2

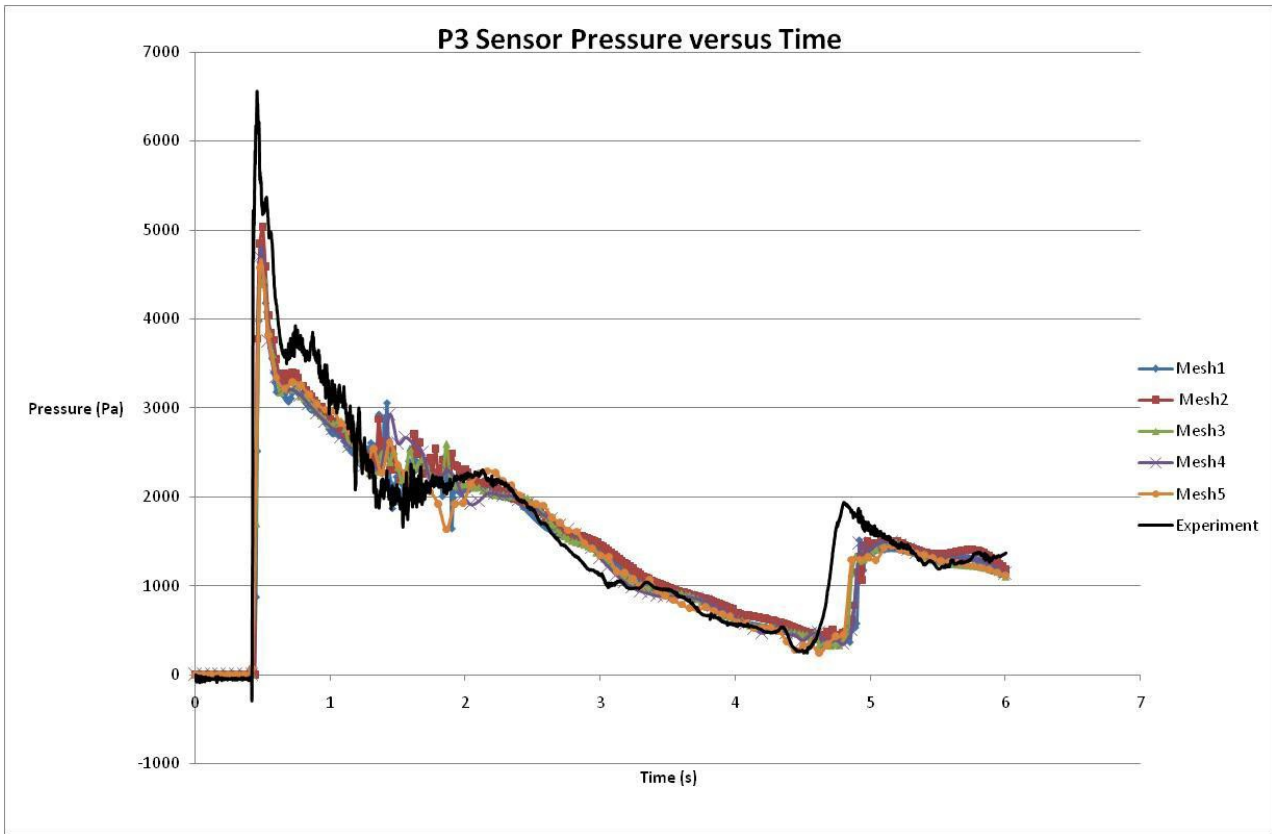


**Figure 9.** Pressure at location P3

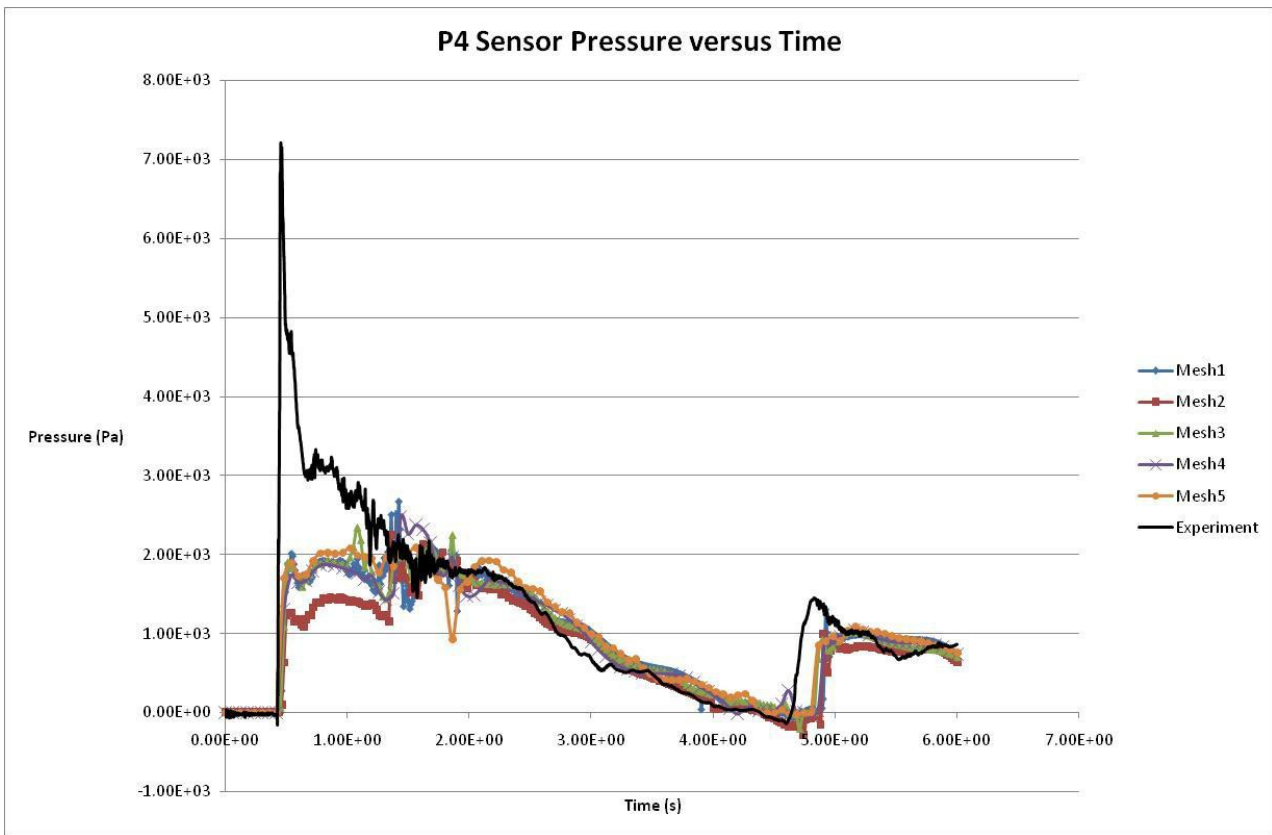


**Figure 10.** Pressure at location P4

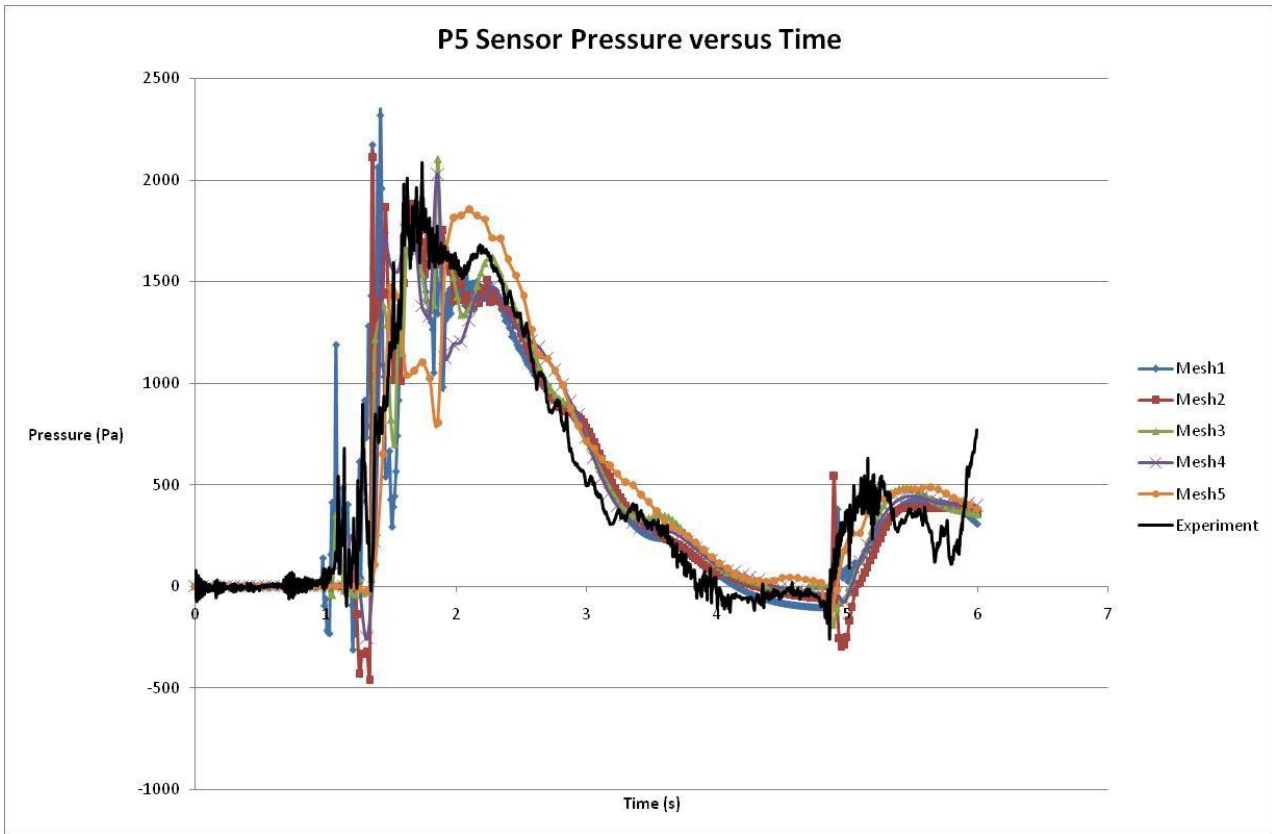


**Figure 11.** Pressure at location P5

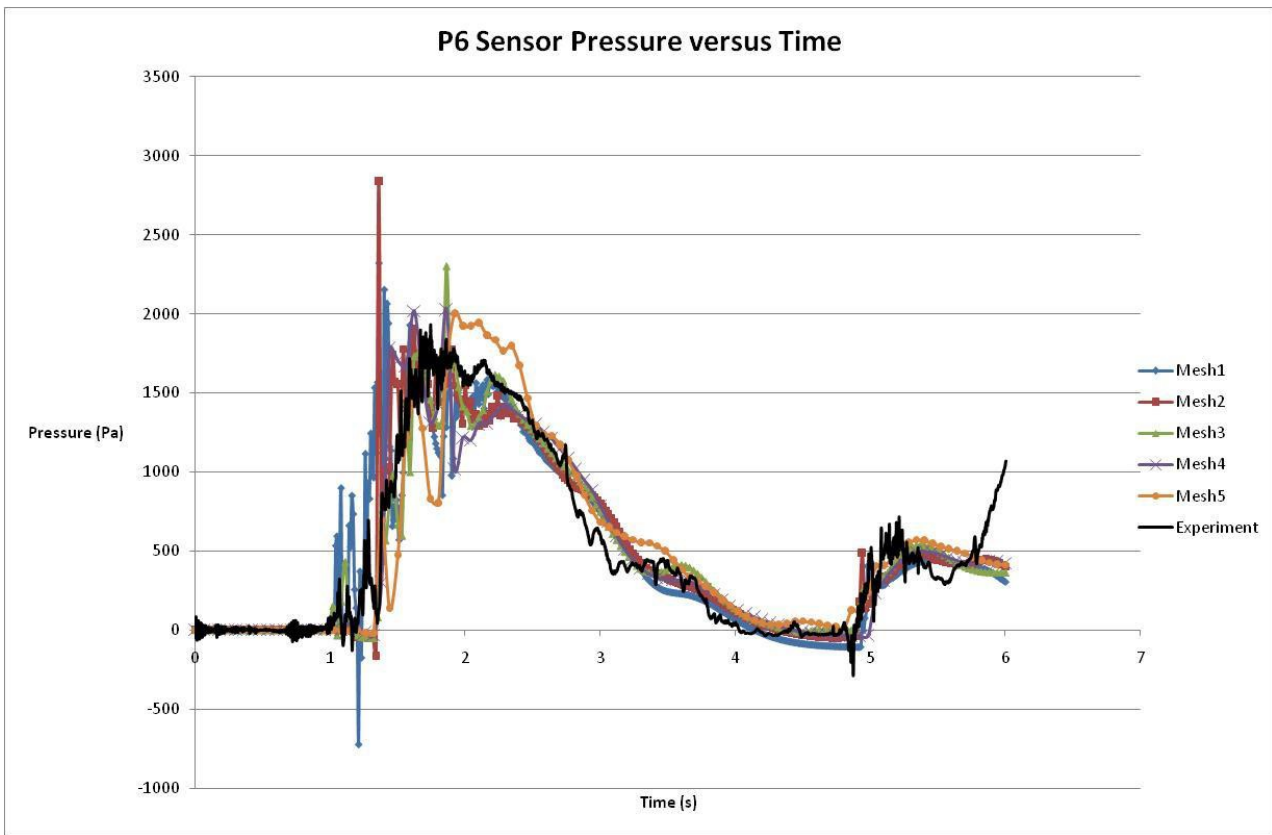


**Figure 12.** Pressure at location P6

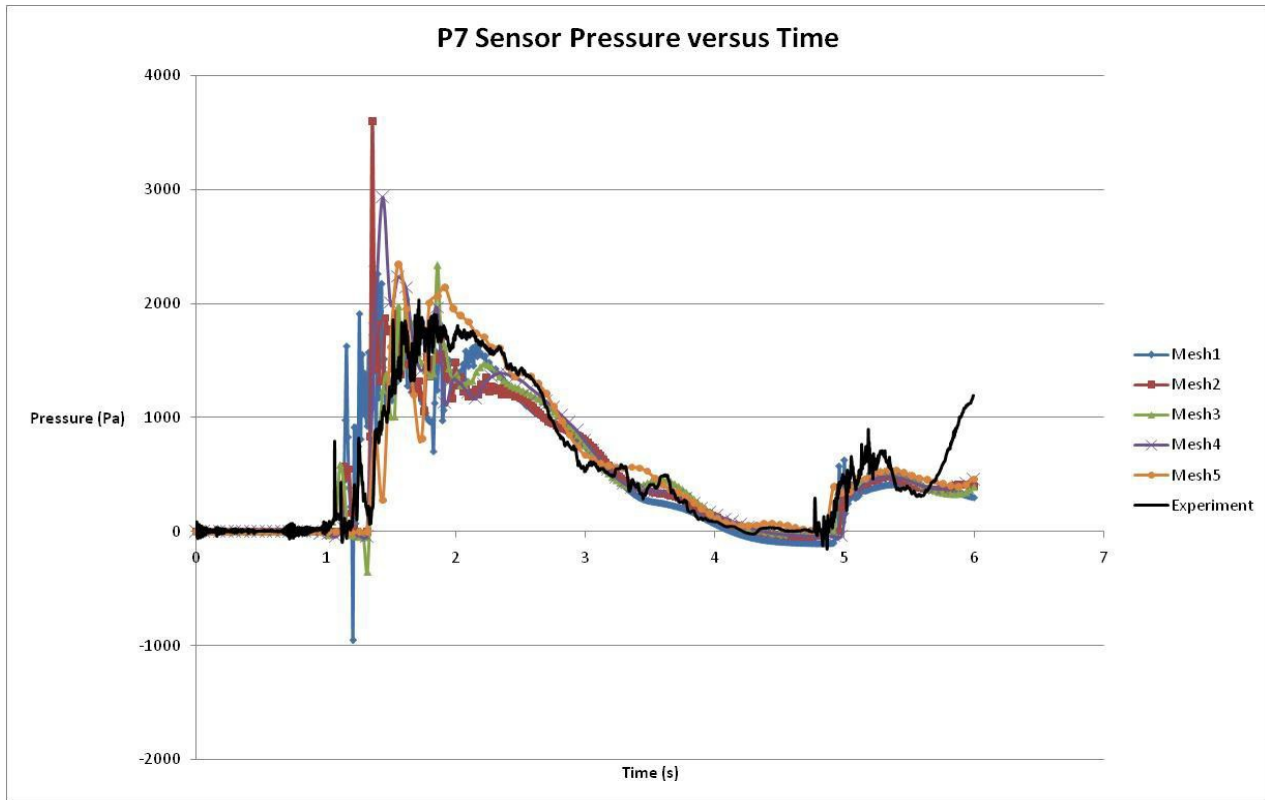


**Figure 13.** Pressure at location P7

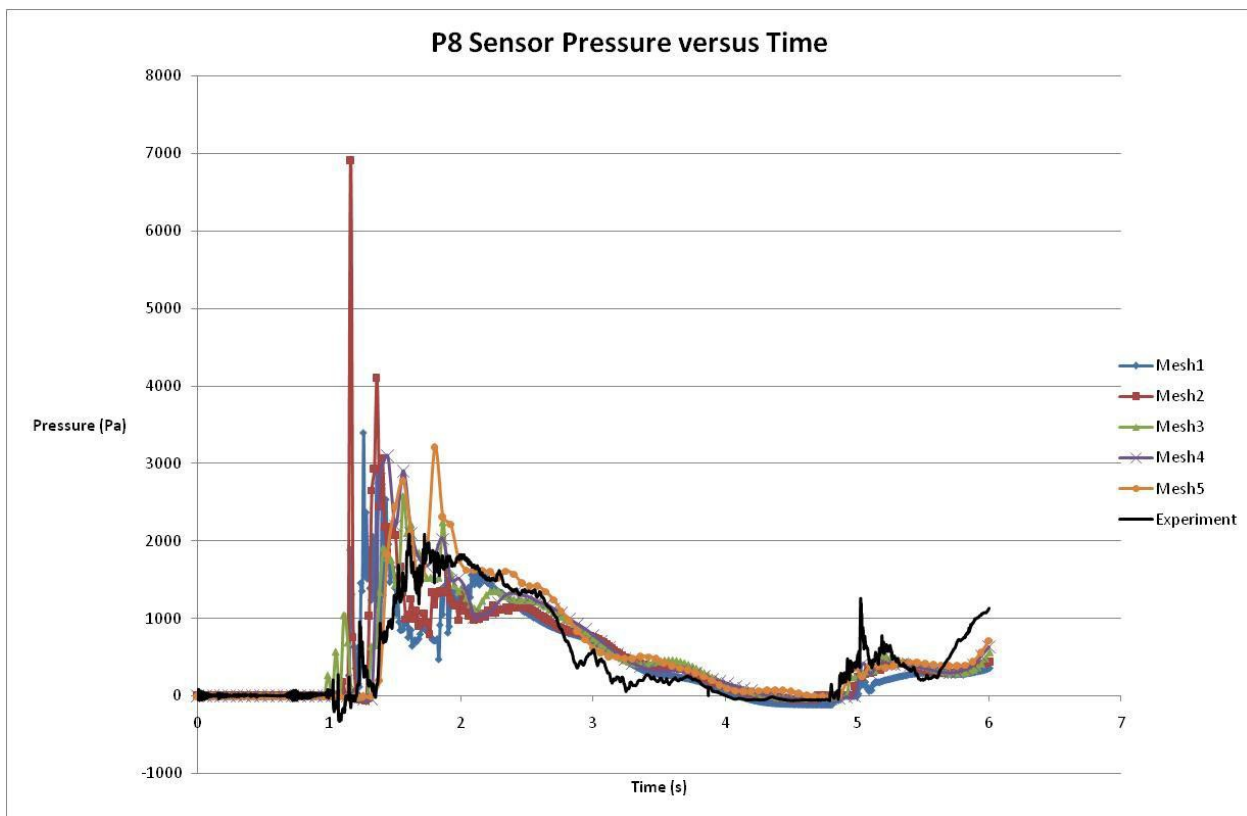


**Figure 14.** Pressure at location P8

## Mesh Refinement

In terms of the effect of mesh refinement there seems to be little evidence that the solution is converging to a unique solution. This is perhaps not surprising as we have attempted to model the turbulence in the flow field by direct simulation instead of using a turbulence model. Using this approach we would expect the time-dependent solution to uncover more detail in the flow field as the mesh is refined and to become more sensitive to perturbations in the initial conditions. Also we would expect the average of many simulations with slightly different initial conditions to converge to an ensemble averaged solution with mesh refinement. However, in terms of the level of agreement with experiment there is little difference between the least and most expensive solutions which took approximately 35 times longer. From an engineering perspective the coarsest mesh solution, i.e., Mesh 1 would be sufficiently accurate and represents very good value considering the elapsed simulation was only just over 15 minutes.

## Order of Numerical Scheme

The effect of the momentum advection numerical scheme order and the effect of running single or double precision arithmetic are shown in figures 15-18. For brevity only the four free-surface height values are shown. The 2nd order and 3rd order schemes show very similar results which both follow the experimental curve a little more closely than the more diffuse 1st order scheme. Also the higher order schemes appear to follow the experimental curve on the coarser Mesh 1 better than the 1st order scheme on Meshes 4 and 5. The double precision curve deviates from the single precision 1st order curve only slightly. Given the relatively small expense of using a higher order scheme and double precision arithmetic it seems logical to do so in future calculations providing stability is not compromised.

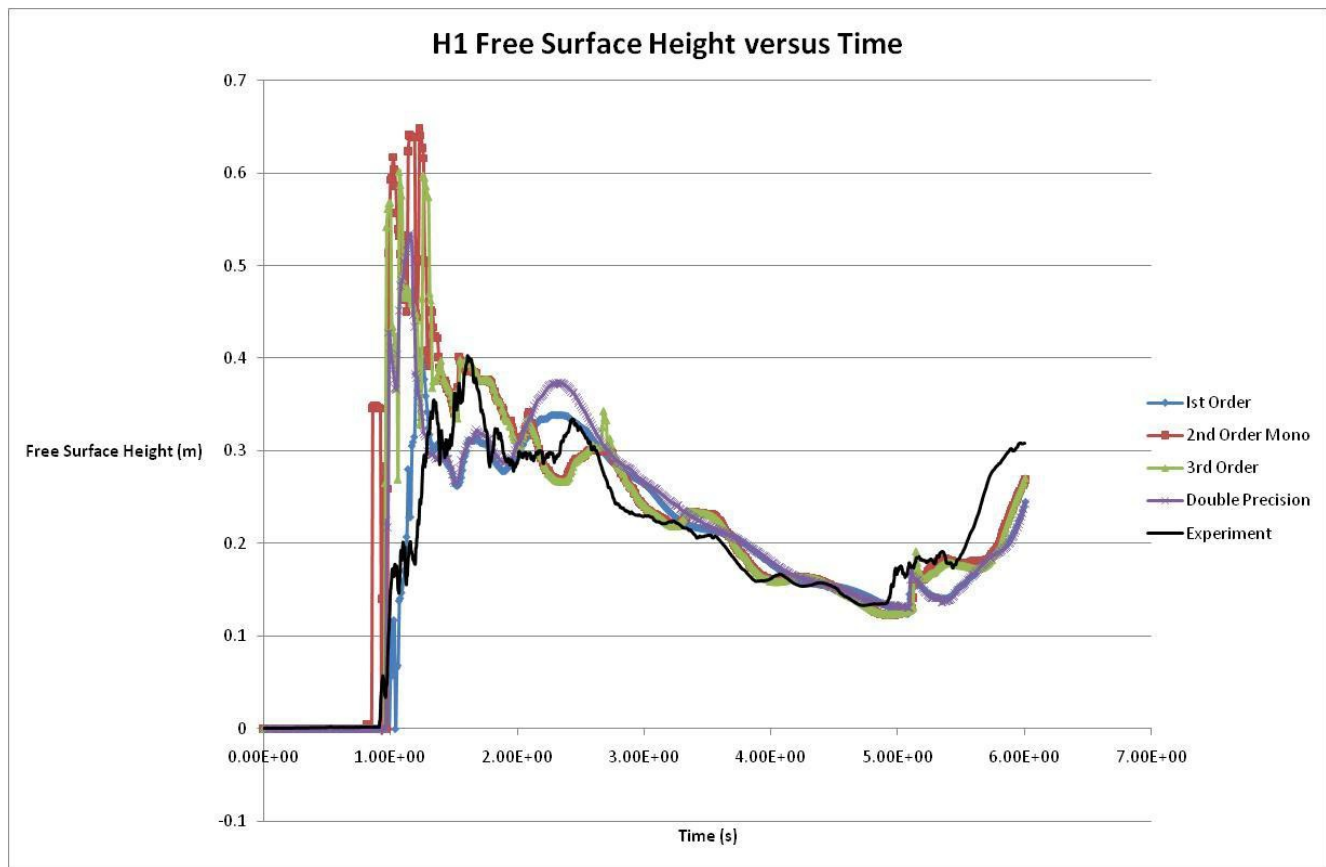


**Figure 15.** Free-surface height at location H1 for various numerical schemes and precision levels

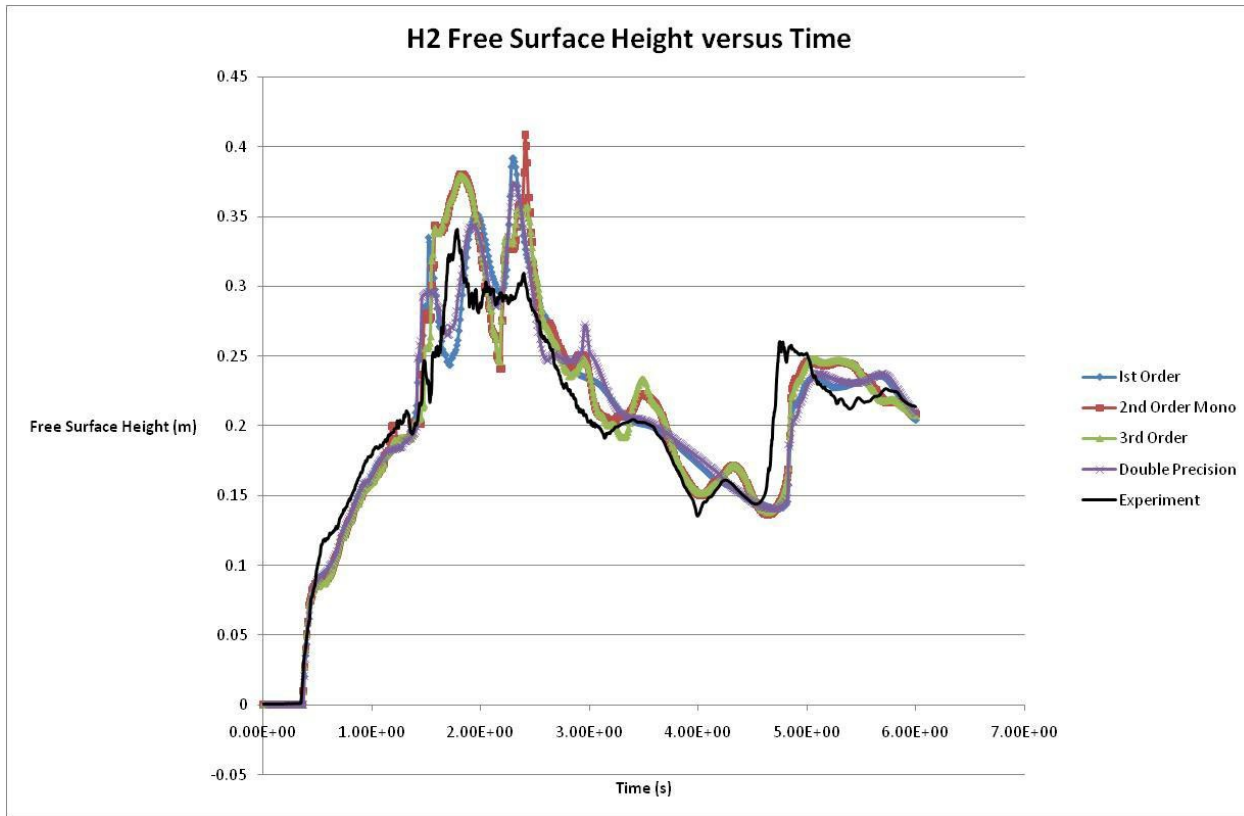


**Figure 16.** Height at location H2 for various numerical schemes and precision levels

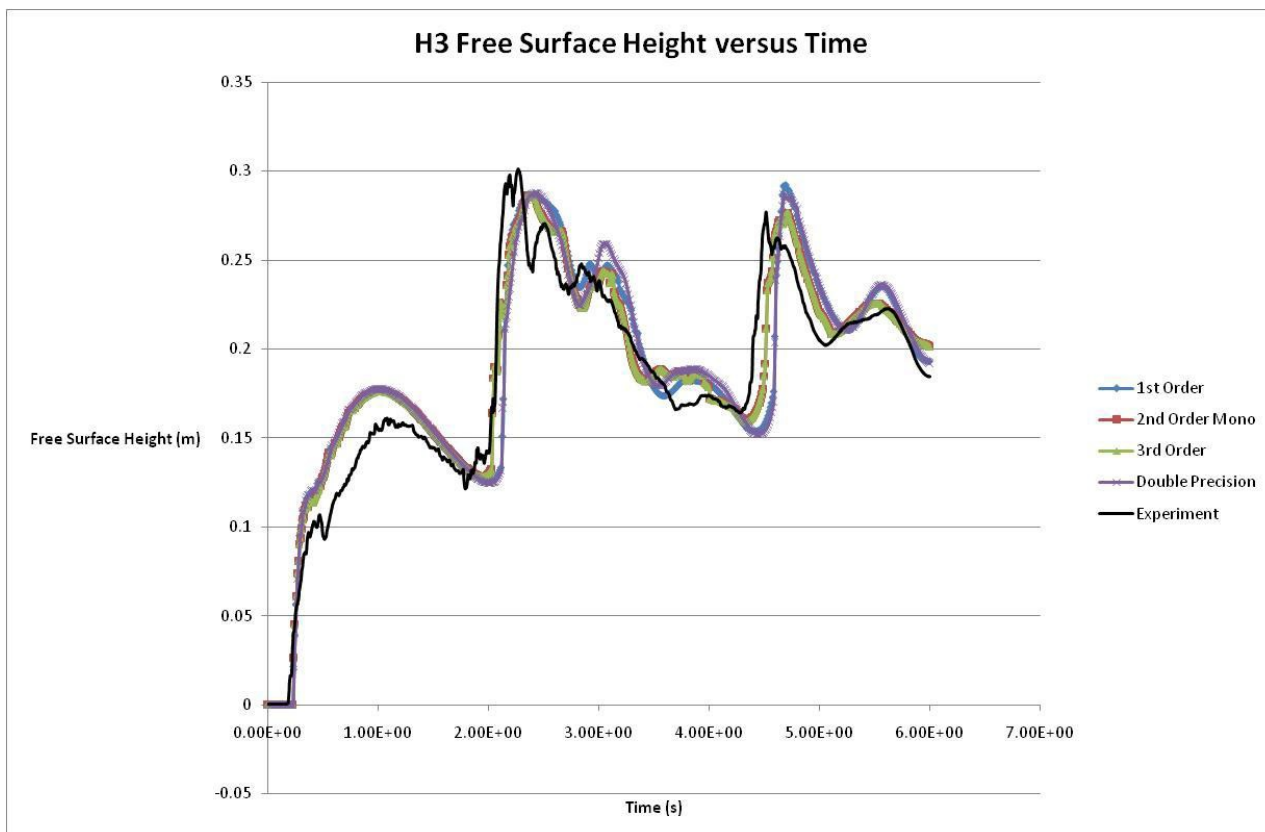


**Figure 17.** Free-surface height at location H3 for various numerical schemes and precision levels

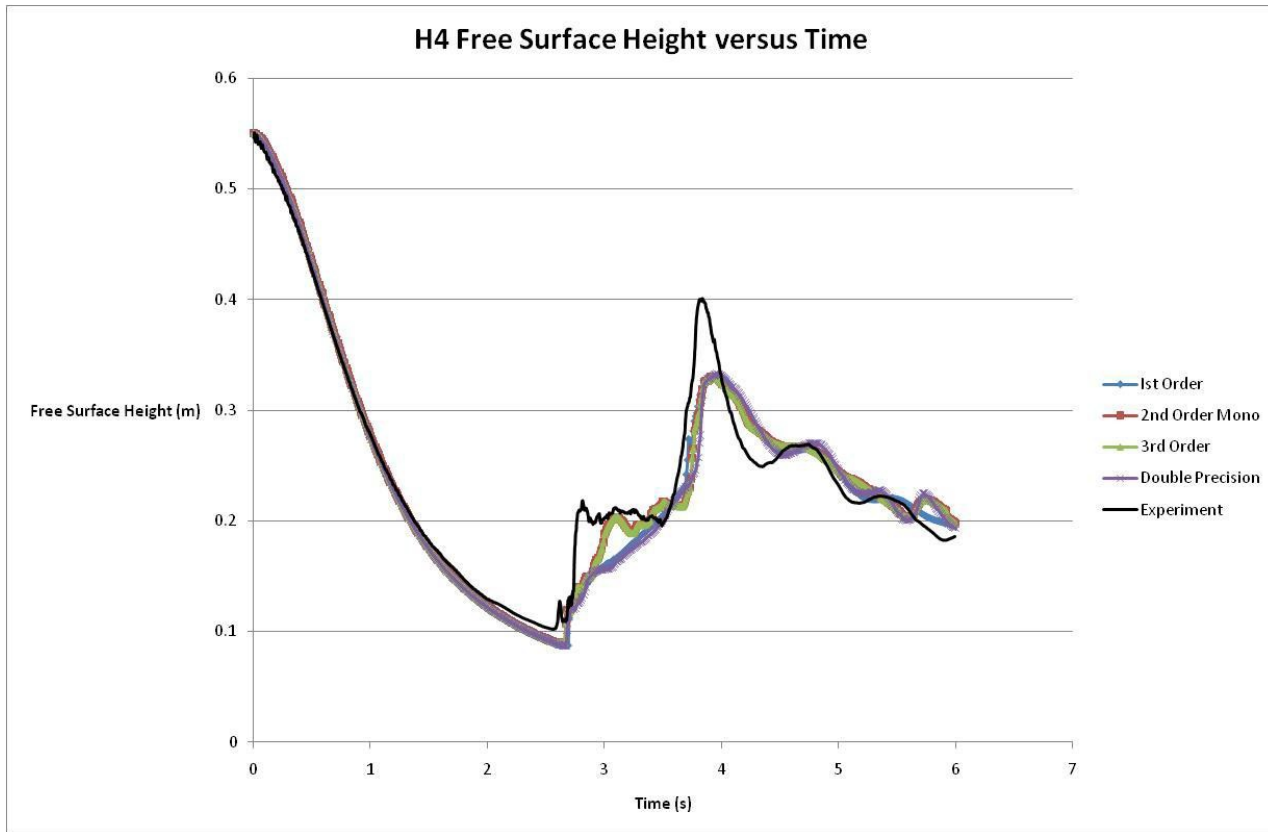


**Figure 18.** Free-surface height at location H4 for various numerical schemes and precision levels

## Turbulence Model

The effect of the method used to model the turbulent fluctuations is shown in figures 19 to 22. For brevity only the four free-surface height values are shown. However, from these plots there would appear to be no clear winner in terms of each models' ability to more accurately predict the experimental time histories. The CPU times for each model are given in table 1 and show the LES model to be almost as economical as the laminar model compared to almost twice as long for the more conventional RNG formulation.

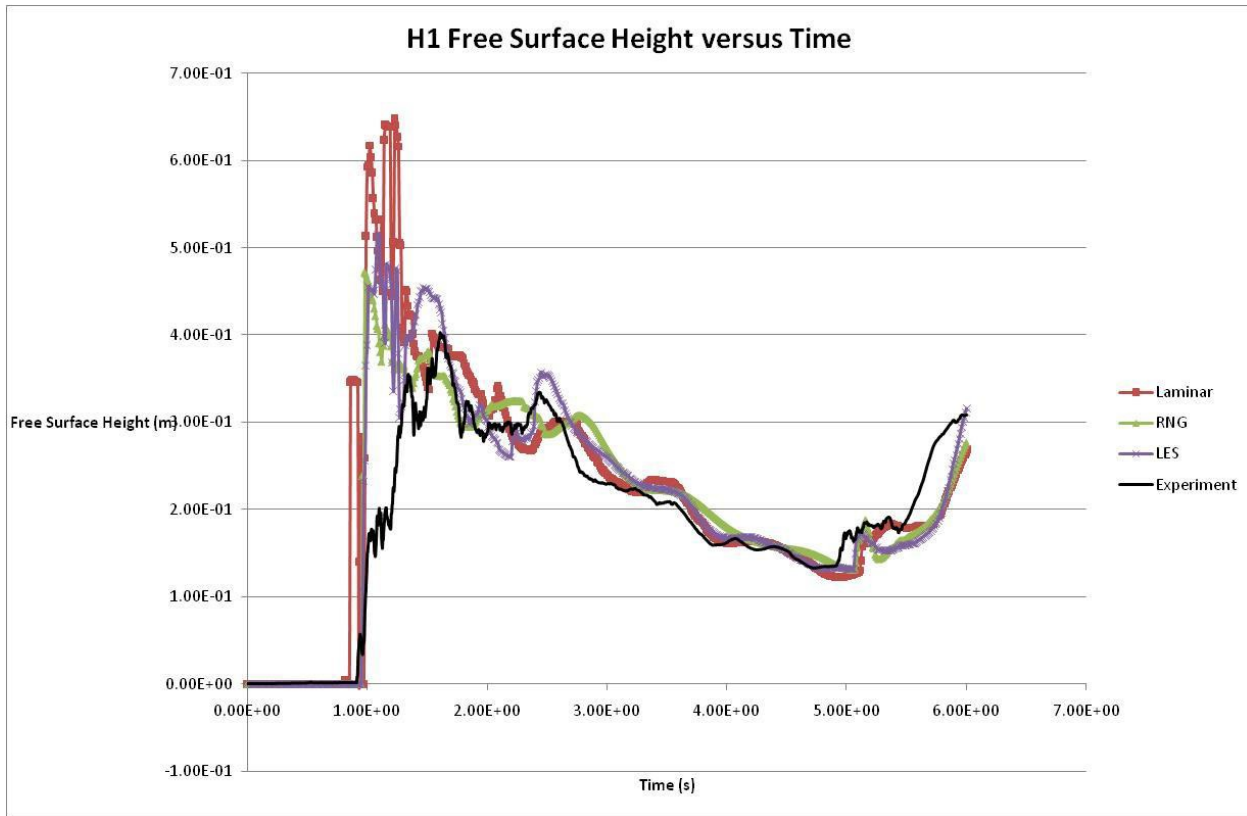


**Figure 19.** Free-surface height at location H1 for various turbulence models

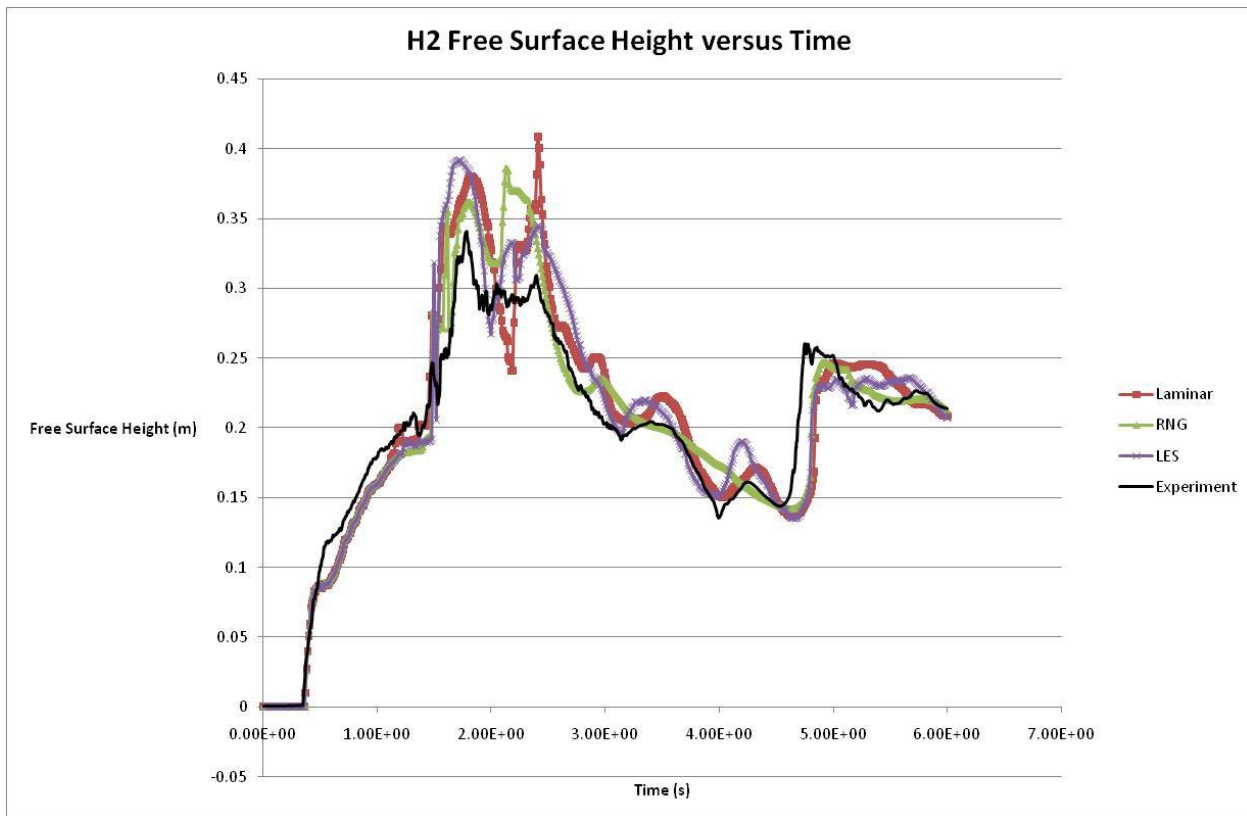


**Figure 20.** Free-surface height at location H2 for various turbulence models

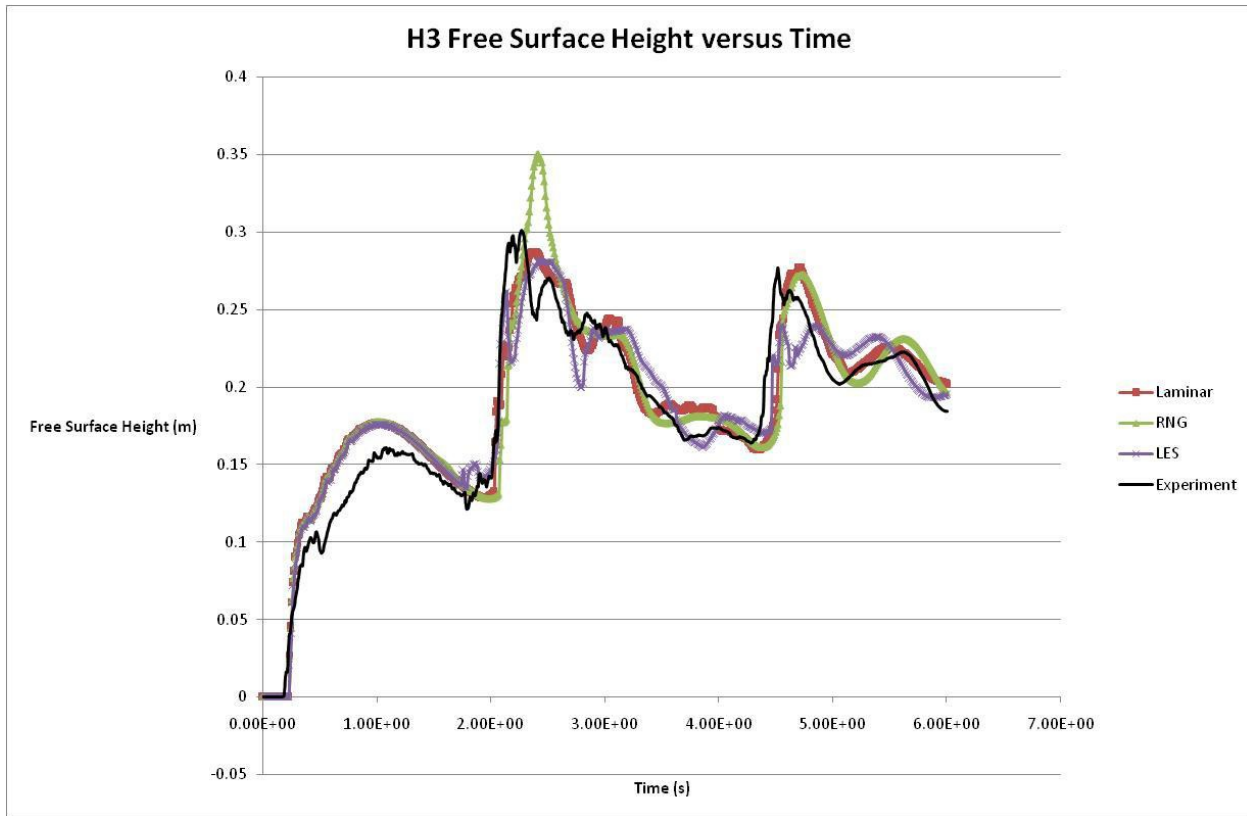


**Figure 21.** Free-surface height at location H3 for various turbulence models

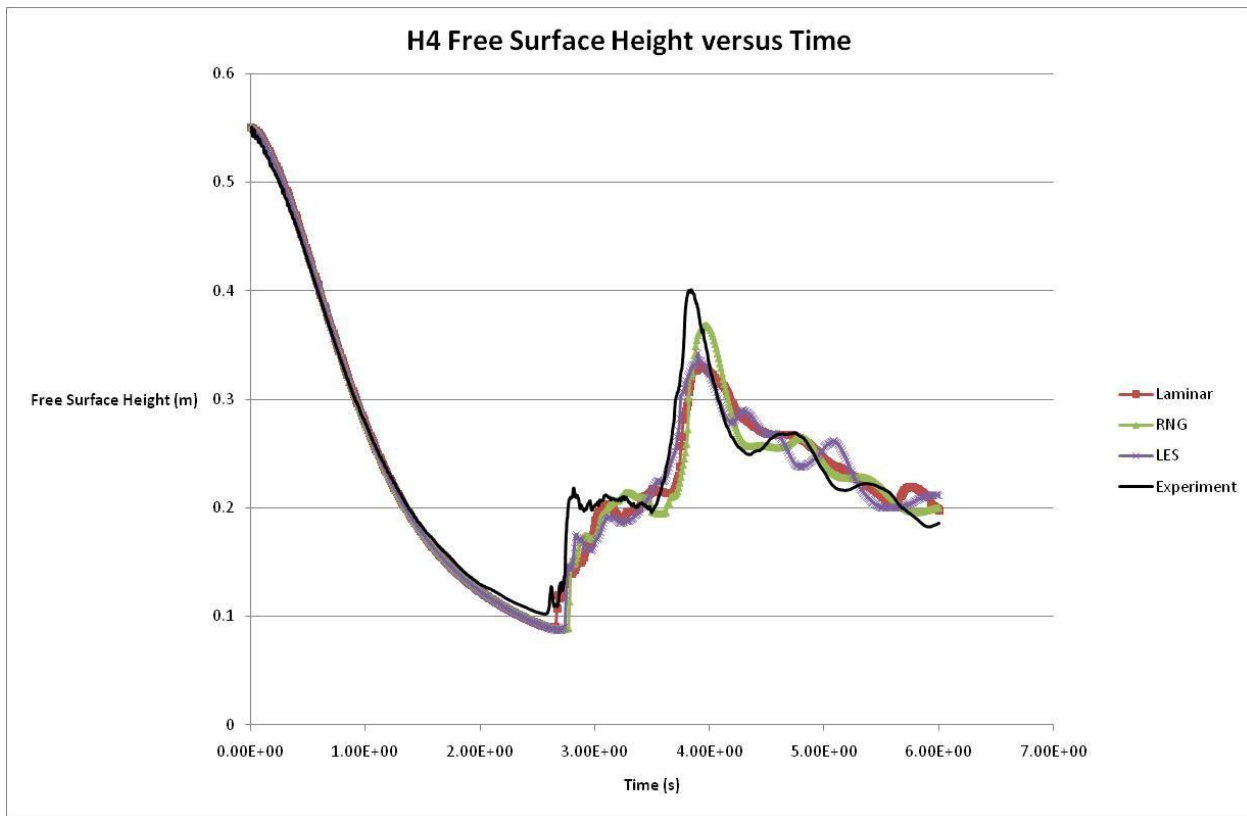


**Figure 22.** Free-surface height at location H4 for various turbulence models

## Conclusion

**FLOW-3D** has been used to simulate a very challenging free-surface flow problem and has produced good qualitative and quantitative agreement with the experimental data. The main discrepancies could easily be due to problems measuring the free-surface elevation of what is at times a non-unique parameter. The prediction of pressure on the surface of an obstacle on which the flow impinges is also generally in good agreement with the experimental measurement, the main deviation being again where there is a significant amount of fluctuation in the experimental measurements. The repeatability of the experimental measurements has not been discussed in the literature but is likely to be at least as large as the differences in the CFD simulations. We have also found that the solution can be adequately obtained on a relatively coarse mesh using 1st order differencing with no turbulence model in around 15 minutes on a shared memory configuration over four processors. The lack of need for a turbulence model suggests that the turbulent structures which dominate the resulting flow are resolvable at this level of mesh refinement.

## Acknowledgements

The author gratefully acknowledges the funding provided by Wavebob Limited, which enabled this work to be completed.

## References

1. SPH European Research Interest Community SIG, R.Issa and D. Violeau, *Test-Case 2 3D dam breaking*, <http://wiki.manchester.ac.uk/spheric/index.php/Test2>
2. K.M.T Kleefsman, G. Fekken, A.E P Veldman, B. Iwanowski, and B. Buchner, *A volume of fluid based simulation method for wave impact problems*, J Comp Phs, 206: 363-393, 2005.